1 **Cycling hypoxia selects for constitutive HIF stabilization**
2
3 Mariyah Pressley[1], Jill A. Gallaher[1], Joel S. Brown[1], Michal R. Tomaszewski[2], Punit Borad[2],
4 Mehdi Damaghi[2], Robert J. Gillies[2], Christopher J. Whelan[2*]
5
6 [1]Department of Integrated Mathematical Oncology, Moffitt Cancer Center and Research Institute,
7 Tampa, FL 33612 USA
8
9 [2]Department of Cancer Physiology, Moffitt Cancer Center and Research Institute, Tampa, FL
10 33612 USA
11
12 **Running Title: Selection for constitutive HIF stabilization**
13
14 **Keywords:** Hypoxia, Fluctuating oxygen concentrations, Normoxia, Optimal defense theory,
15 Pseudohypoxia
16
17 **Additional Information**
18 **Word count:**

19 Main text: 4,358; Abstract: 147; Methods: 1,444

20 Number figures: 7; Number tables: 1

21
22 ***Corresponding author**
23 Christopher J Whelan
24 Email: chris.whelan@moffitt.org
25 Phone: +1 6304505960; Fax: 813-745-8053
26 Address: Moffitt Cancer Center & Research Institute
27 SRB4, 12902 Magnolia Drive
28 Tampa, FL 33612 USA
29
30
31

Abstract

Tumors experience temporal and spatial fluctuations in oxygenation. Hypoxia inducible transcription factors (HIF-α) in tumor cells are stabilized in response to low levels of oxygen and induce angiogenesis to re-supply oxygen. HIF-α stabilization is typically facultative, induced by hypoxia and reduced by normoxia. In some cancers, however, HIF-α stabilization becomes constitutive even under normoxia, a condition known as *pseudohypoxia*. Herein, we develop a mathematical model that predicts the effects of fluctuating levels of oxygen availability on stabilization of HIF-α and its client proteins based on fitness. The model shows that facultative regulation of HIF-α always promotes greater cell fitness than constitutive regulation. However, cell fitness is nearly identical regardless of HIF-α regulation strategy when there are rapid periodic fluctuations in oxygenation. Furthermore, the model predicts that stochastic changes in oxygenation favor facultative HIF-α regulation. We conclude that rapid and regular cycling of oxygenation levels selects for pseudohypoxia.

Introduction

Phenotypic plasticity, the production of alternative phenotypes in response to variable environments, is ubiquitous in nature[1]. Phenotypic plasticity confers flexibility that allows an organism to survive in the face of often unpredictable and rapid changes in its environment. Many organisms, from microbes to humans, vary gene expression facultatively. In this way phenotypic expression matches demand[2,3]. In contrast, when environments are constant, or are predictably variable, an intermediate and constitutive level of expression may be favored over facultative expression[4,5].

Inducible or facultative defenses, such as defensive chemicals in plants, and spines and projections in zooplankton such as rotifers and cladocerans, include remarkably diverse and well-studied examples of phenotypically plastic responses to biotic and abiotic threats or stressors. Biotic threats include herbivores, predators, pathogens and parasites. An important abiotic threat is hypoxia, a reduction in oxygen availability. Hypoxia may be either acute, intermittent, or chronic, and it may be experienced at the organismal, tissue, or cellular levels. Cells respond to hypoxia via stabilization of the Hypoxia-inducible Factor (HIF), an inducible defense against both acute and chronic hypoxia within the cellular environment. HIF is a heterodimeric transcription factor that induces expression of genes that lead to tissue re-oxygenation. The evolution of inducible defenses, like HIF, appears to be favored by unpredictability of environmental conditions, reliable cues of those conditions, and a high cost of the defense[6-8].

Oxygen levels in normoxic or hypoxic tissues encompass a wide range of values depending on several factors, including gender, time of day, tissue type, and degree of vascularization[9,10]. In tumors, significant heterogeneity in oxygen levels result from both a dynamic ecosystem of blood vessels of varying functionality, and cancer cells with different tolerances to hypoxia. Within a nascent tumor ecosystem, cancer cells, which can somatically evolve, experience both acute and chronic hypoxia due to rapid growth, limited blood supply, and disorganized vascular delivery systems[11]. This leads to complex cycles of oxygenation and hypoxia, characterized as "waves" and "tides"[12-14]. Thus, an intermittent or temporal instability in oxygen supply is a cardinal feature of tumors. We have proposed that this generates strong evolutionary selection pressures for more aggressive cancer cell phenotypes[15].

2

78   Like nearly all metazoan cells, cancer cells possess mechanisms to respond to
79 heterogeneity in the supply of oxygen, including activation of a family of hypoxia-inducible
80 transcription factors (HIF-1α, HIF-2α, and HIF-3α; hereafter HIF-α), cell cycle arrest, a
81 coordinated decrease in oxidative phosphorylation with an increase in glycolysis (Pasteur Effect),
82 and the secretion of angiogenic factors to promote blood vessel formation[16-21]. HIF-α is
83 ubiquitously and continuously expressed in all cells. In well-oxygenated environments (normoxia),
84 HIF-α is hydroxylated and ubiquitinated and is thus recognized and degraded by proteasomes[19].
85 In an oxygen-depleted state, hydroxylation and hence, degradation of HIF-α is inhibited,
86 promoting the transcription of genes that regulate proliferation[22,23], cellular metabolism[19],
87 angiogenesis[24] and erythropoiesis[25-26]. If well-regulated, the recruitment of blood vessels to the
88 site of HIF-α stabilization increases the supply of oxygen. Once O_2 levels return to normal
89 (normoxia), HIF-α returns to baseline levels. It has also been observed that aggressive cancers
90 constitutively express hypoxia-related proteins (HRPs) even in the presence of oxygen, a condition
91 known as *pseudohypoxia*[27]. The most common manifestation of this phenotype is the fermentation
92 of glucose under normoxia, known as "aerobic glycolysis" or the "Warburg Effect"[28-30].
93
94   Maintenance of HIF-α levels under cycling hypoxia involves tradeoffs. Under prolonged
95 hypoxia without stabilization of HIF-α, cells die. In contrast, HIF-α stabilization under normoxia
96 comes at a cost. Accumulation of HIF-α in well-oxygenated environments costs energy and
97 resources for the synthesis of HIF-α client proteins that may not be necessary for survival,
98 including activating energetically inefficient glycolysis and expression of the exofacial acidifying
99 pH-stat, carbonic anhydrase isoform 9, CA-IX[31]. As seen in the development of some tumors,
100 regulation of HIF-α switches from a facultative state, where the environment induces the changes
101 in regulation, to a constitutive state, where HIF-α and/or HIF-α client proteins remain above
102 baseline regardless of the environment[15,27]. As this phenotype is associated with cancer progression
103 and aggressiveness, understanding the microenvironmental conditions that select for
104 pseudohypoxia is fundamentally important.
105
106   Here, we develop a mathematical model with the goal of determining a cancer cell's
107 optimal level of HIF-α expression with respect to differences in fluctuating levels of oxygen
108 availability within tumor microenvironments. Specifically, we seek to determine what tumor
109 conditions may cause the evolution of constitutive HIF-α regulation ("hard wired" HIF-α
110 stabilization) from facultative regulation. To do so we compare the maximal expected payoff (net
111 growth rate) between facultative and constitutive HIF-α regulation in environments with different
112 oxygen profiles. We hypothesize that predictable and rapid cyclic fluctuations from normoxia to
113 hypoxia will favor constitutive HIF-α stabilization based on similar ideas in optimal defense
114 theory[4,32].
115
116   Our model investigates how cells may respond to changes in oxygenation with HIF-α
117 expression. In a perfect world, cells would instantaneously optimize HIF-α levels in response to
118 fluctuating oxygen concentrations. As the environment shifts from normoxia to hypoxia, cells
119 would immediately accumulate HIF-α, and vice-versa. However, attaining the appropriate HIF-α
120 level for the current environment is not immediate. There will be time lags in upregulating or down
121 regulating HIF-α. HIF-α production and proteosomal degradation occur continuously[18,27]. When
122 oxygenation levels decline, HIF-α degradation slows, and production permits HIF-α to increase at
123 a relatively slow rate to counter the hypoxic conditions[18]. Upon re-oxygenation, HIF-α can be

124 rapidly degraded. We model cellular regulation of HIF-α as the concentration of oxygen within
125 the tumor and surrounding microenvironment changes temporally – both with regular periodicity
126 and stochastically. The model was informed by empirical evidence for the rates of HIF-α
127 accumulation and degradation as the cells' microenvironment shifts between normoxia and
128 hypoxia, and vice-versa[33-35].
129
Results
131 We compared how different HIF-α regulation strategies influence cell fitness under different
132 oxygenation environments. Here, we define a cell's fitness by its net proliferation rate, or "payoff".
133 In this model, we assume that the expected payoff depends on the base proliferation rate, the
134 metabolic cost of expressing HIF-α, and the mortality risk of not expressing HIF-α during hypoxia.
135 We use the following expression for a cancer cell's payoff at time t, $G(t)$:
136

$$G(t) = r - cu(t) - \frac{m(1-q)}{k+bu(t)}, \qquad (1)$$

138

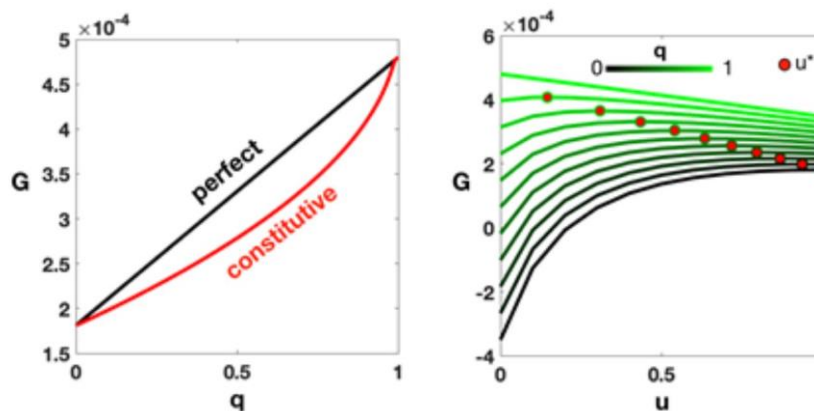| Parameter	Description	Units	Values	References
r	Baseline proliferation rate of a cell	min^{-1}	0.00048	Estimated
c	Cost to proliferation rate when using strategy u	min^{-1}	0.0001328	Calculated
m	Hypoxia induced cell death rate	min^{-1}	0.00083	Guo et al. 2009
k	Cell tolerance to hypoxia in the absence of HIF-α stabilization	unitless	1	Set
b	Cell benefit in hypoxic environments due to HIF-α stabilization	unitless	4	Guo et al. 2009
α_0	Upregulation rate of HIF-α	min^{-1}	0.01155	Pagé et al. 2002
α_1	Downregulation rate of HIF-α	min^{-1}	0.0462	Marxsen et al. 2004
u_{min}	Baseline production of HIF-α	unitless	[0,1]	Optimized
u_{max}	Maximum production of HIF-α	unitless	[0,1]	Optimized
u	HIF-α expression	unitless	[0,1]	Calculated
Y	Level of oxygenation	unitless	[0,1]	Variable
q	Fraction of time the environment is fully oxygenated (Y=1)	min^{-1}	[0,1]	Variable

139
140 Table 1. Definitions, units, and values of parameters used in the models. The terms Y and u are normalized and are therefore
141 unitless. We normalize k to 1 because it appears as m/k when u=0 and appears as b/k in u^*. The value of c is calculated such that
142 $u^* = 1$ when the environment is hypoxic (q=0; $c = \frac{m}{b\left(1+\frac{k}{b}\right)^2}$).

143

144   where r is the baseline proliferation rate of a cancer cell, c is proliferation cost of using HIF-α
145   strategy u at time t, m is the cell mortality when conditions are hypoxic, q is the fraction of time
146   spent in normoxic conditions, k is a cell's intrinsic tolerance to hypoxia in the absence of HIF-α
147   stabilization, and b is the benefit of HIF-α expression u in reducing mortality when conditions
148   are hypoxic. See Table 1 for definitions, units and values of all parameters used in the models.
149

150   We compare three HIF-α strategies across a variety of oxygenation environments:
151   perfect, constitutive, and facultative. A perfect strategy means instantaneous HIF-α switching in
152   response to normoxic and hypoxic conditions. While this strategy is idealized, it provides a
153   useful point of comparison for the other strategies as a perfect strategy would yield the highest
154   possible payoff. A constitutive strategy assumes that the HIF-α level is constant over time, and a
155   facultative strategy assumes that the HIF-α levels can change at a finite rate in response to
156   oxygen levels. Representative examples of these strategies in a fluctuating environment are
157   shown in the Methods (Fig. 7).
158

159   **The perfect strategy**
160   A perfect strategy does not mean perfect fitness in all environments. Mortality and the metabolic
161   costs of HIF-α stabilization means that fitness declines with more time spent in hypoxic conditions.
162   The expected payoff of the perfect strategy (see Eq. (2) in Methods) is shown to decline linearly
163   with the proportion of time spent in hypoxia (Fig. 1A).
164

165

166

Figure 1. Expected payoffs for perfect and constitutive strategies. A) The payoff (G) for perfect and optimal constitutive (u^*) strategies for different fractions of time in normoxic conditions, q. B) The payoff versus HIF-α level, u, for different q's. The lines represent all u values, while the red dots represent the optimal u expression (u^*) for each q that maximizes the payoff. Parameter values are given in Table 1.

167

168

169   **The constitutive strategy**
170   The optimal constitutive strategy can be found by maximizing the payoff for a constant HIF-α
171   level, u^* (see Eq. (3) in Methods). The expression for the payoff can then be analytically solved
172   (see Eq. (4) in Methods). We found that the constitutive strategy payoff is always less than or
173   equal to the perfect strategy payoff (Fig. 1A), being equal only when the environment is always
174   hypoxic ($q = 0$) or always normoxic ($q = 1$). The payoff over different HIF-α regulation strategy
175   values u for different fractions of time spent in normoxia q is plotted in Fig. 1B, along with the
176   optimal constitutive values u^*. As expected, we find that the payoff is highest when HIF-α

177   expression is lowest (u=0) under constant normoxic conditions. With constant normoxia, as u is
178   increased, the payoff slightly decreases, showing the minor cost of unnecessarily producing HIF-
179   α. However, as conditions become more hypoxic with a low HIF-α expression, the mortality
180   term dominates, and the payoff is drastically reduced into negative values where the cell cannot
181   survive. With constant hypoxia, HIF-α needs to increase in order for $G \geq 0$ for survival. The
182   optimal values u*, shown as red dots, reflect this for all values of q in between.
183
184   **Facultative expression of HIF-α**
185   With the facultative strategy, u changes over time according to Eq. (5) in the Methods. This
186   expression allows u to increase in hypoxia and decrease in normoxia at the rates given in Table 1.
187   The rates were based on empirical measurements[33-35], which found that HIF-α down-regulation
188   occurs about four times faster than HIF-α up-regulation. The optimal facultative strategy involves
189   selecting a baseline u_{min} and an upper bound u_{max} that maximizes the expected payoff. For
190   simulations we began with a period of normoxia and a starting value of HIF-α halfway between
191   constitutive expression and the specified u_{max}. For fixed cycle lengths, the expected payoff
192   converges quickly to a steady state, and we use the payoff in Eq. (6) in the Methods to numerically
193   solve for the optimal lower and upper bounds of u^*_{min} and an upper bound u^*_{max}.
194
195   We compared the optimal facultative response between two different periodicities (either
196   10 minute or 120 minute intervals) of full oxygenation followed by the same for deoxygenation (q
197   = 0.5 in both cases). Initially we compared the payoffs of a constitutive strategy and facultative
198   strategy in the same environment to determine the selection coefficient, which we defined as the
199   fitness advantage for using a facultative strategy (details in the Methods). The selection
200   coefficients over the full range of possible u_{min} and u_{max} are shown in Fig. 2A. For longer cycling
201   periods, the facultative strategy has a larger selection coefficient for any given combination of u_{min}
202   and u_{max} than for shorter cycle times. Under many circumstances the difference in the selection
203   coefficients for the two strategies are so small as to be negligible. Under such circumstances one
204   might expect the constitutive strategy to prevail.
205
206   We further explored HIF-α expression using the u_{min} and u_{max} combination that produced
207   the greatest payoff. When the environment fluctuates with time intervals of 10 minutes, the cell's
208   payoff was optimized at u^*_{min}=0.540 and u^*_{max}=1. The fluctuation in HIF-α expression occurred
209   rapidly and the u^*_{min}, while always less than, came close to the constitutive value, while u^*_{max}
210   remained at 1 (Fig. 2B). By increasing time intervals to 120 minutes, the cell's payoff was
211   maximized at u^*_{min}=0.305 and u^*_{max}=1. The longer cycle times resulted in larger fluctuations in
212   HIF-α expression and a greater superiority of the facultative strategy compared to the constitutive
213   strategy. With the longer cycle time, the optimal facultative strategy resulted in a lower value for
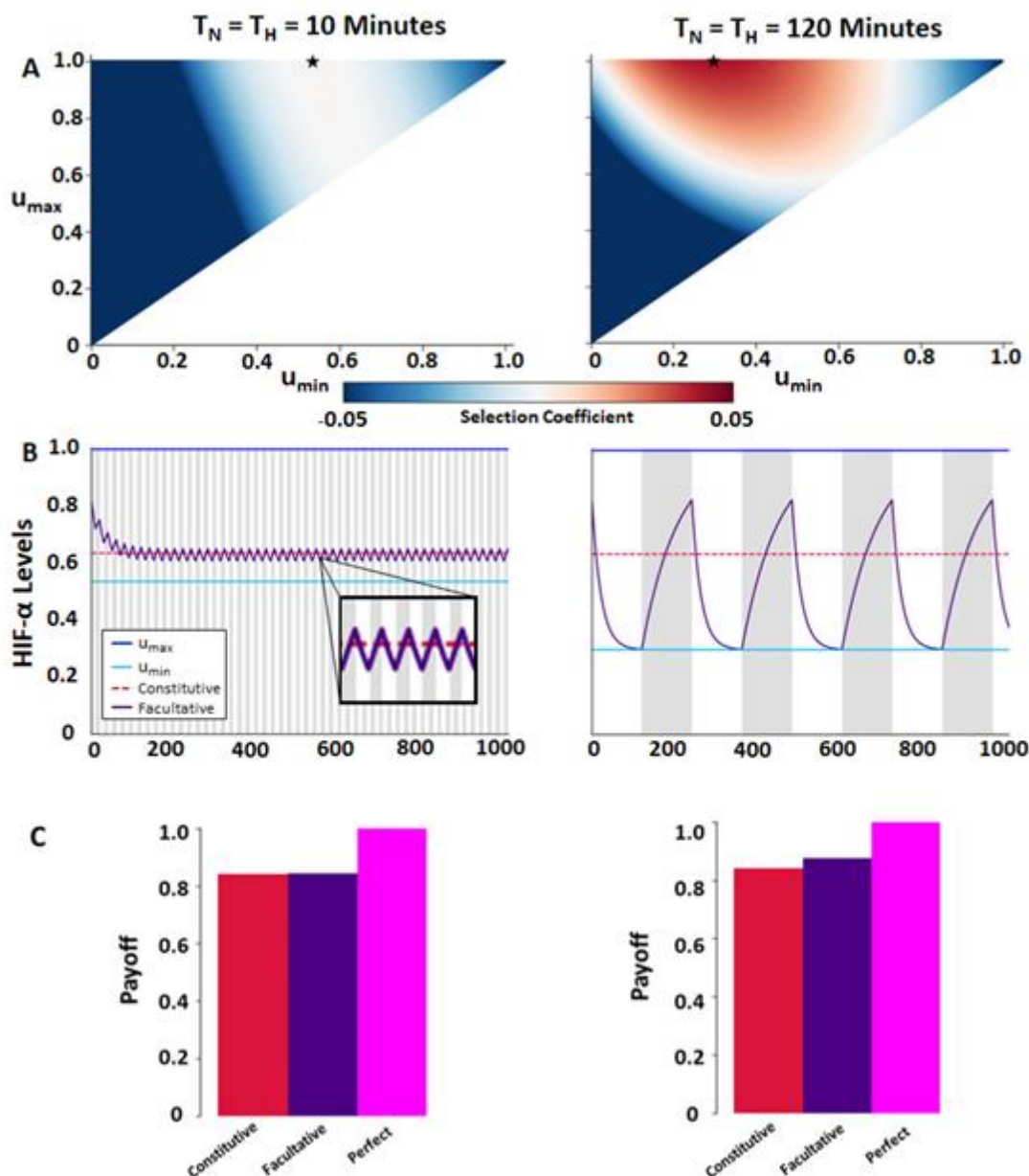214 u^*_{min}, while u^*_{max} always remained at 1.
215

6

Figure 2. Comparison environments with fixed intervals of short (10 min) and long (120 min) periods of cycling hypoxia. A) Heatmap of the selection coefficients for the facultative strategy for all u_{min} and u_{max} combinations. Each star denotes the u_{min} and u_{max} combination that maximizes payoffs for the facultative strategy for each fixed interval time. B) HIF-α (u) levels over time using the optimal facultative strategy. The unshaded areas represent periods of full oxygenation while the shaded grey areas represent periods of hypoxia. C) Payoffs for separate strategies of HIF-α expression normalized to the perfect strategy. Parameters are given in Table 1.

Comparing over all strategies, we found that perfect matching of HIF-α expression to fluctuating levels of oxygenation always produces the highest cell payoff (Fig. 2C). However, for facultative and constitutive strategies that work on non-instantaneous time scales, we found that the superiority of the facultative over the constitutive strategy was low for short cycles and high for longer cycles.

HIF-α expression under stochastic fluctuations

For stochastic oxygen fluctuations, we convert the cycle times to rates of switching and use these probabilities to create a timeline of stochastic fluctuations comparable to the fractions of time spent in each environment. Specifically, we let $P_{N \to H} = 1/T_N$ be the probability of switching from normoxia to hypoxia, and $P_{H \to N} = 1/T_H$ be the probability of switching from hypoxia to normoxia, and we evaluated the facultative strategy in stochastic environments where $P_{N \to H} = P_{H \to N}$.
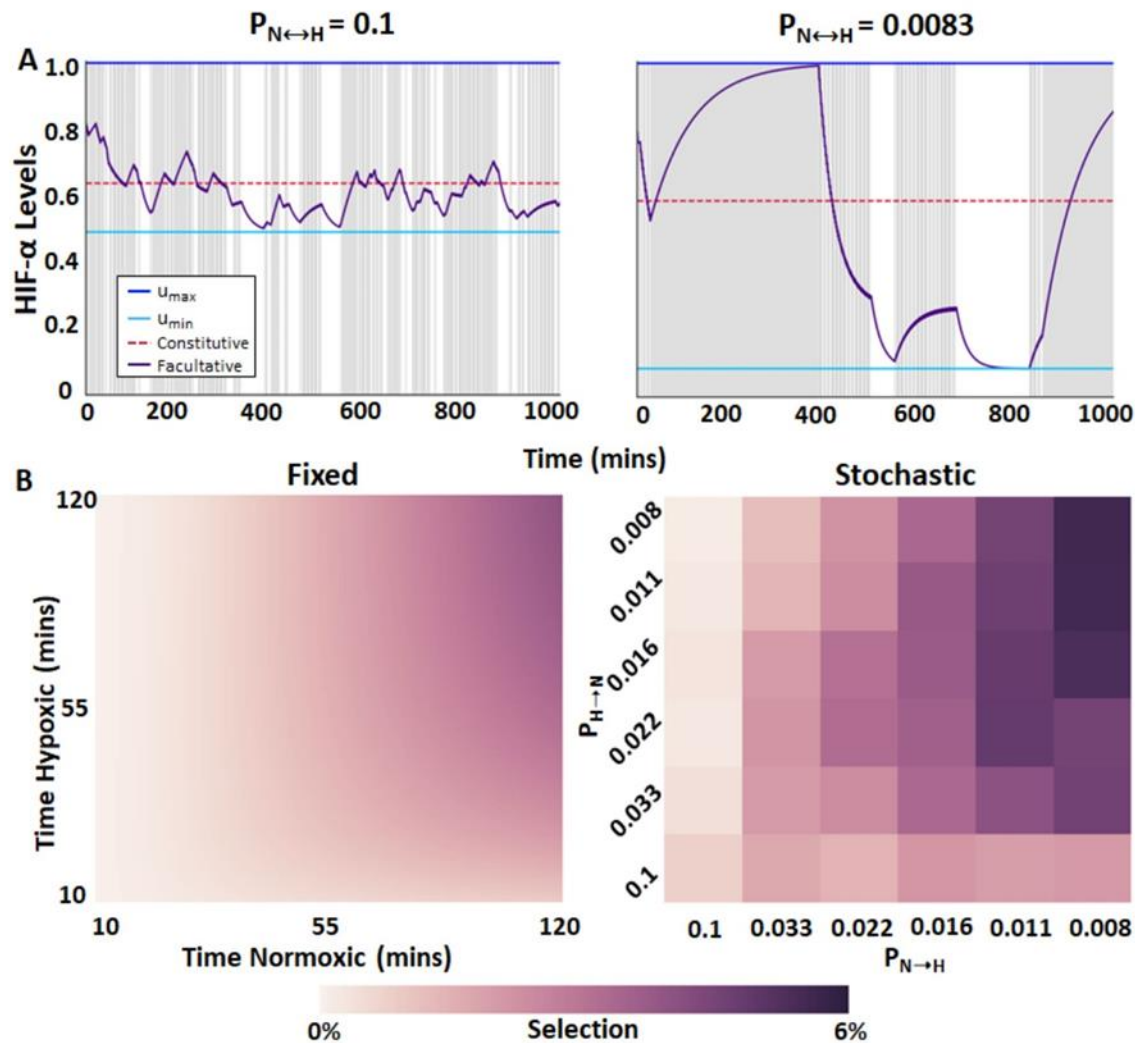

Figure 3. HIF-α regulation under stochastic fluctuations in oxygenation. A) Optimal facultative HIF-α expression in stochastically hypoxic environment; r = 0.00048, α_0=0.01155, α_1=0.0462, m = 0.00083, b = 4, c = 0.0001328, and k=1. Left graph illustrates HIF-α stabilization when the probability of fluctuations in oxygenation states is high (P=0.1) and low (P=0.0083). B) Selection for a facultative strategy over a constitutive strategy for fixed interval and stochastic environments. Because selection is optimized numerically in fixed interval environments, selection gradient is continuous. Selection in stochastic environments is presented as the average of 10 simulation results.

An example simulation with a high probability of switching (left) and a low probability of switching (right) is shown in Fig. 3A. When there is a high probability of switching oxygenation states, $P_{N \to H} = P_{H \to N} = 0.1$ min^{-1}, the optimal facultative strategy occurs at u^*_{min}= 0.504 and u^*_{max}

8

269   = 1. Decreasing the probability of switching to 0.0083 min^{-1} leads to a decrease in $u*_{min}$ to 0.216,
270   while $u*_{max}$ remains unchanged at 1. For comparison, when $P_{N \rightarrow H} = P_{H \rightarrow N}$, assuming $q = 0.5$, the
271   optimal constitutive strategy is u*=0.634. All results for stochastic switching are reported as the
272   mean values of $u*_{min}$ and $u*_{max}$ for 10 simulations insuring a small standard error (<0.01) for $u*_{min}$
273   and $u*_{max}$, respectively (Suppl. Fig. 1).
274

275   **Quantification of stabilization/de-stabilization times in vitro**
276   In the simulations above, we needed estimates for the rates of upregulation and downregulation of
277   HIF-α. We used average rates based on values in the literature from both normal and cancer cell
278   lines. Yet, such rates will vary with cell line and the values from the literature were not collected
279   with our model in mind. To compare to previous values and to our model, we empirically
280   measured HIF-α upregulation and downregulation rates in two different ovarian cancer cell lines,
281   TOV112D and A2780s. The kinetics of HIF-α stabilization were measured under 0.2% hypoxia *in*
282   *vitro*. For TOV112D, HIF-α upregulation and stabilization required at least one hour and was
283   maximal at 4 hours (Fig. 4A, left panel). For A2780s cells, stabilization required 4 hours (Fig. 4A,
284   right panel). We then measured the length of time required for these cancer cell lines to return to
285   normal HIF-α expression after being exposed to hypoxic conditions for 72 hours. After restoring
286   normoxia, TOV112D returned to normal HIF-α expression in about one minute (Fig. 4B left),
287   while A2780 cells returned to normal HIF-α expression in about five minutes (Fig. 4B right). These
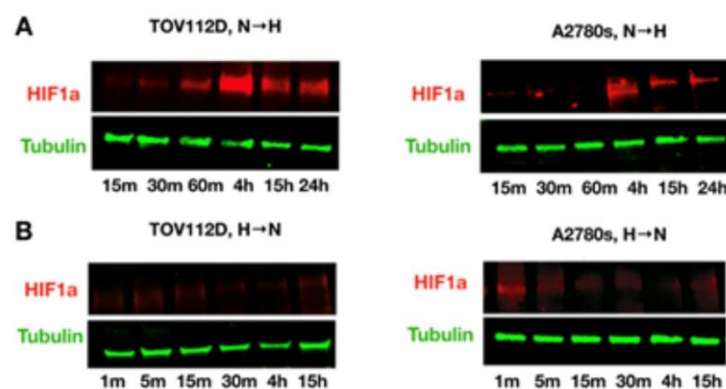288   are significantly more rapid than prior reports (33-35).
289

Figure 4. Quantification of HIF-1α stabilization/de-stabilization times in vitro. Using two ovarian cancer cell lines, HIF-1α expression is found in whole lysate by Western blot analysis. Tubulin is used as control of loading the same amount of proteins. A) To measure the stabilization time, cancer cells were cultured in separate dishes, incubated in hypoxia chambers, and collected at several time points. B) To measure the destabilization time, cancer cells were grown for 72h under hypoxia, and collected at several time points after switching to normoxic conditions. See Methods for more details.

290
291

292   We then estimated the upregulation (α_0) and downregulation (α_1) rates of HIF-α. Using
293   Eqs. (S1) and (S2), and assuming that $u_{max}=1$, $u_{min}=0$, we estimated the rate of upregulation of HIF-
294   *a* by finding values of α_0 that would allow HIF-α to increase to 90% of its maximum stabilization
295   values (in arbitrary units) in 60 minutes and 240 minutes for TOV112D and A2780 cells,
296   respectively. Similarly, we estimated the rate of HIF-α downregulation by finding values of α_1 that
297   allow HIF-*a* to decline to 10% of its maximum stabilization values within 1 minute and 5 minutes
298   for TOV112D and A2780 cells, respectively. These yielded estimates for $\alpha_0 \sim 0.038$ min^{-1} for
299   TOV112D and $\alpha_0 \sim 0.01$ min^{-1} for A2780 and estimates of $\alpha_1 \sim 2.3$ min^{-1} for TOV112D and $\alpha_1 \sim 0.46$
300   min^{-1} for A2780. We incorporated these experimentally derived rates into the model to compare
301   the facultative and constitutive strategies in fixed interval environments. As with our previous
302   results, we find greater selection for a facultative strategy in environments that remain in their
303   current state of oxygenation or lack thereof for longer time periods. The superiority of the
304   facultative strategy over the constitutive depends heavily on up- and down-regulation rates.

305 Decreasing the rate at which HIF-α accumulates reduces the advantage of being facultative over
306 constitutive even in environments with longer cycles. In general, the model suggests that
307 TOV112D cells should exhibit a facultative strategy and A2780 cells a constitutive (see Suppl.
308 Fig. 2).
309
310 **Oxygen fluctuations in vivo**
311 Intra-tumoral fluctuations in oxygenation are key for empirically evaluating whether a constitutive
312 strategy may be favored over a facultative one. Furthermore, fluctuations within a tumor may vary
313 spatially. Thus, different regions of a tumor may select for different HIF-α levels and strategies.
314 To gain empirical insights, we measured spatio-temporal variation in oxygen delivery in different
315 regions of a mouse pancreatic adenocarcinoma tumor. We used *in vivo* MR quantification of
316 dynamic T2* changes. Significant heterogeneity was observed within the tumor both in the mean
317 (Fig. 5A) and the temporal variance (Fig. 5B) of T2* values, indicating areas of variable blood
318 flow and oxygenation. The temporal profiles of fluctuations were distinct in different areas, and
319 consistent with different blood vessels feeding these regions. Interestingly, while random, short
320 fluctuations were observed in some areas (Fig. 5C), some displayed changes at much longer time
321 scales (Fig. 5D) in both directions of normoxia to hypoxia and hypoxia to normoxia. We might
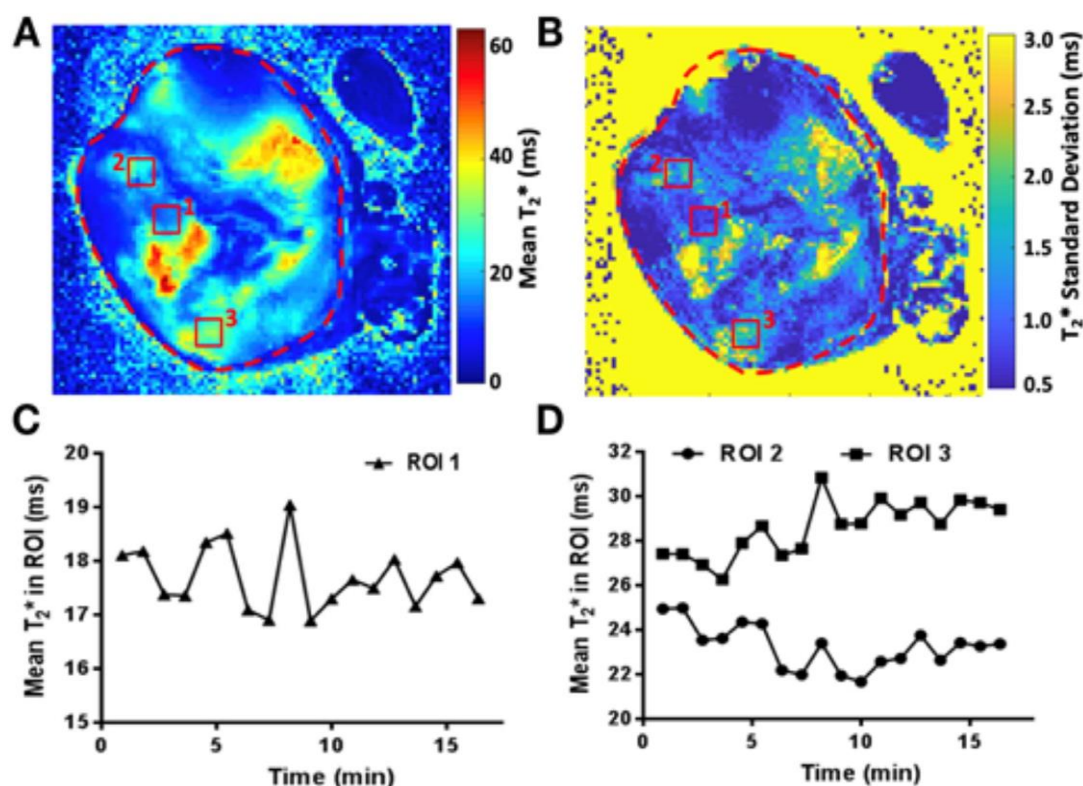322 expect a constitutive strategy to be favored in the former regions and facultative in the latter.
323

Figure 5. Oxygen fluctuations in vivo. A) Mean T2* value and B) standard deviation of the T2* changes in time are shown for a representative slice. Small regions of interest, marked with red rectangles, were drawn to illustrate distinct temporal T2* kinetics in tumor, plotted in C (ROI 1) and D (ROI 2s and 3).

10

Discussion

324
325 Facultative regulation of HIF-α in response to fluctuating levels of oxygenation is ancestral and
326 highly conserved across phyla[36-38]. For this reason, the evolution of constitutive HIF-α regulation
327 has drawn wide interest across many biological disciplines, including cancer. Herein, we
328 developed a theoretical model to explore the conditions under which constitutive versus facultative
329 HIF-α orchestration of the cellular response to temporal changes in oxygen supply will optimize a
330 cell's fitness, as measured by the net growth rate, or payoff. Our modeling indicates,
331 unsurprisingly, that the perfect matching strategy for HIF-α regulation in response to fluctuating
332 oxygenation levels always delivers a greater payoff than either the facultative or the constitutive
333 strategies. However, cellular transcriptional and translational machinery has significant inertia and
334 is unable to instantaneously respond to fluctuations in oxygenation and thus unable to provide a
335 perfect match. Thus, it must respond either facultatively or constitutively. Under facultative
336 regulation, the upper and lower bounds for rates of HIF accumulation are critical for calibrating
337 the rate at which the cancer cells stabilize their oxygen environment. Our model predicts that the
338 upper bound should be set very high to rapidly respond to hypoxia. Conversely the lower bound
339 insures a non-zero level of stabilization. This increased baseline level of stabilization for the
340 facultative strategy is only slightly below what would be expected with constitutive regulation of
341 HIF-α. Importantly, this demonstrates the larger penalty of not upregulating HIF-α quickly enough
342 when the environment becomes hypoxic than the cost incurred of needlessly stabilizing HIF-α
343 during normoxia. Thus, cells constitutively expressing HIF-α may be at a selective advantage
344 under some conditions, with little cost.

345
346   Our model indicates that facultative expression of HIF-α always promotes a greater payoff
347 than constitutive expression. Importantly, however, the difference in the payoffs between
348 facultative and constitutive HIF-α expression depends on the nature of the fluctuations between
349 normoxia and hypoxia. With short cycling times, the difference between facultative and
350 constitutive HIF-α stabilization is small and perhaps negligible, so facultative expression may be
351 indistinguishable from constitutive regulation. In contrast, long cycling times or stochastic
352 fluctuations favor facultative HIF-α regulation.

353
354   Our modeling results match expectations from nature. For instance, plants rely on inducible
355 (facultative) and/or constitutive defenses against herbivores or pathogens. Optimal defense theory
356 (ODT)[4,32] predicts deployment strategies for these plant defenses. ODT states that: (1) defenses
357 should be preferentially invested in those tissues that most affect individual fitness, and (2) the
358 reliance on an inducible defense should depend on the probability or predictability of attack (Fig.
359 6). When the probability of attack is low, there should be greater reliance on inducible versus
360 constitutive defense, and vice-versa when the probability of attack is high. Indeed, as the
361 probability of attack nears 100%, ODT states that fitness is maximized when defenses are
362 constitutive.

363
364   Applying this reasoning to HIF-α expression under cyclic hypoxia, fixed periodicities with
365 rapid fluctuations of oxygenation equate to a 100% certainty that a cell will experience hypoxia[39].
366 Hence, ODT predicts that cells should regulate HIF-α expression constitutively. In our simulations,
367 when oxygenation states switch rapidly at fixed intervals, we found that payoffs are virtually
368 identical between facultative and constitutive HIF-α regulation (Fig 2C). When fluctuations are
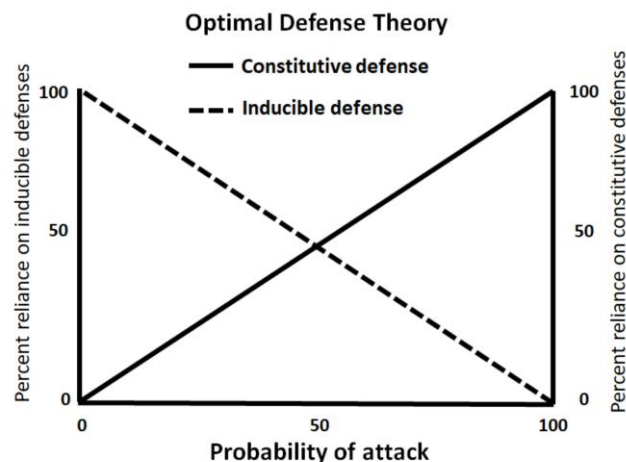
11

369

Figure 6. Optimal defense theory. Optimal defense theory predicts that tissues with a low probability of being attacked should rely primarily on inducible defenses, whereas those with a high probability of attack should rely primarily on constitutive defenses.

370   fixed, and with short periods of normoxia interspersed between long periods of hypoxia, the
371   selective advantage of facultative HIF-α regulation is only slightly greater than with constitutive
372   HIF-α regulation (Fig. 3B). Under both scenarios, any mutation that results in constitutive HIF-α
373   regulation (e.g. mutations in VHL ubiquitin ligase) will be selectively permissive, i.e. it will not
374   be strongly selected against. We speculate that the loss of VHL observed in renal cell cancer
375   implies a constitutive response strategy due to rapid fluctuations in oxygenation early in its
376   development. Cells with a mutation that results in constitutive HIF-α regulation will thus be able
377   to coexist with cells with facultative HIF-α regulation. This mirrors the case in many tumors, in
378   which some cells express the wild-type (normal) HIF-α phenotype (facultative HIF regulation),
379   and some cells express the Warburg phenotype (constitutive HIF-α regulation). Our modeling also
380   suggests that cells evolving under rapid switches in oxygenation may retain facultative HIF-α
381   regulation, but they may set their upper and lower bounds of HIF-α in a way that is effectively
382   pseudohypoxic (Fig. 2B). Under these conditions, the distinction between facultative and
383   constitutive HIF-α regulation becomes moot.

384

385   With stochastic fluctuations in oxygenation states, in contrast, the probability of hypoxia
386   is less certain or predictable. Then, as predicted with ODT, facultative HIF-α regulation should be
387   favored. In our simulations, stochastic changes in oxygenation always resulted in greater selection
388   coefficients for facultative relative to constitutive HIF-α stabilization (Fig 3B). Under this
389   scenario, cells with mutations that produce constitutive HIF-α regulation will be less fit than cells
390   with facultative HIF-α regulation, and these cells would be eliminated or reduced to a minor
391   population through competition.

392

393   The imaging results presented provide *in vivo* insight into the dynamics of tumor oxygen
394   environment through indirect measurements of blood oxygen level changes in the local vascular
395   network. The apparent fluctuations observed highlight the importance of understanding the cellular
396   mechanisms of adaptation to dynamic conditions. In particular, the measured spatial heterogeneity
397   of the temporal profiles suggests likely coexistence of the different HIF-α regulation strategies
398   within one tumor. With intra-tumoral variation in oxygenation regimes, we expect not only to see
399   variation in the level of HIF-α expression but also the coexistence of cancer cells exhibiting

400 different HIF-α strategies. In the future, spatial relationships can be incorporated into our model
401 to elucidate the nature of these interactions.
402
403   Our review of the literature on the dynamics of up- and down-regulation rates, and
404 confirmed by our own experiments indicate that HIF-α response dynamics vary considerably
405 between experimental cell lines (our results above)[33-35]. These differences may represent genetic,
406 epigenetic, or phenotypically plastic differences among tissue types within organisms[40,41] or
407 evolved differences between species[41,42]. Such heterogeneity may reflect tissue-specific
408 fluctuations in oxygenation, or fluctuations in oxygenation specific to the environments inhabited
409 by different species. This means that cancers initiating from different cell types within different
410 tissues may start with quite varied rates for upregulating and downregulating HIF-α; and these
411 upregulation and downregulation strategies may vary with cancer cell evolution and progression.
412 These differences may later influence the emergence of pseudohypoxia via constitutive HIF-α
413 expression or epigenetic stabilization of downstream products of HIF-α such as CAIX. Of note,
414 though, is the near universality of pseudohypoxia (Warburg Effect) in malignant cancers,
415 indicating that this provides a fitness advantage regardless of the trajectory used to acquire this
416 phenotype[27].
417
418   Previous mathematical models of hypoxia and HIF-α regulation fall into four general
419 categories[43]: (1) understanding the switch-like behavior of the HIF-α response to fluctuating O_2[44];
420 (2) analysis of the role of molecular elements of the microenvironment during the HIF-α
421 response[45]; (3) elaborating how asparaginyl hydroxylase factor inhibiting HIF-1 (FIH) affects the
422 HIF-α response[46-48]); and (4) capturing the temporal dynamics of the HIF-α response[46,48]. All of
423 these modeling studies have helped elucidate the core elements that shape the activity and the
424 dynamics of the HIF-α response to cycling hypoxia. Our model, in contrast, addresses the
425 conditions that select for the evolution of constitutive regulation of HIF-α from the ancestral
426 facultative regulation. Our model examines the consequences of different HIF-α regulation
427 strategies on cell fitness within the complex and dynamic tumor ecosystem. We find that
428 constitutive HIF-α regulation is favored when the probability of hypoxia is high – a finding that is
429 consistent with ecological models of defenses to biotic threats like predation and herbivory.
430
431   The current study is the first of its kind to apply ecological defense theory to the expression
432 of stress responses (e.g. HIF) in cancer cells. Hence, it is not without its limitations. First, the
433 endpoint for our simulations to model fitness was simply net growth rate, as represented by our
434 payoff function. There are many other components to fitness that were not considered in this
435 study. For example, the expression of some pseudohypoxic gene products, e.g. CAIX or VEGF,
436 may confer upon cells additional selection advantages, such as an increased ability to invade and
437 colonize adjacent tissues[49], thus increasing the fitness of the pseudohypoxic phenotype. A second
438 limitation is that the study investigated only the kinetics of stabilizing HIF-1α. There are at least
439 two other HIF-α proteins, each with different activation kinetics and portfolios of client proteins.
440 Moreover, the kinetics of the transcriptional and translational machinery induced by HIF-α are not
441 known with certainty, and presumably do not respond instantaneously. Knowledge generated by
442 investigating these limitations will improve subsequent models.
443
444
445

13

446 **Methods**
447 **Mathematical Model and Major Assumptions**
448 We modeled three different strategies by which a cell can respond to the presence or withdrawal
449 of oxygen in an environment: perfect, constitutive, and facultative (Fig. 7). If a cell responds
450 perfectly to an environment, the fluctuating oxygen profile would be matched by the cell
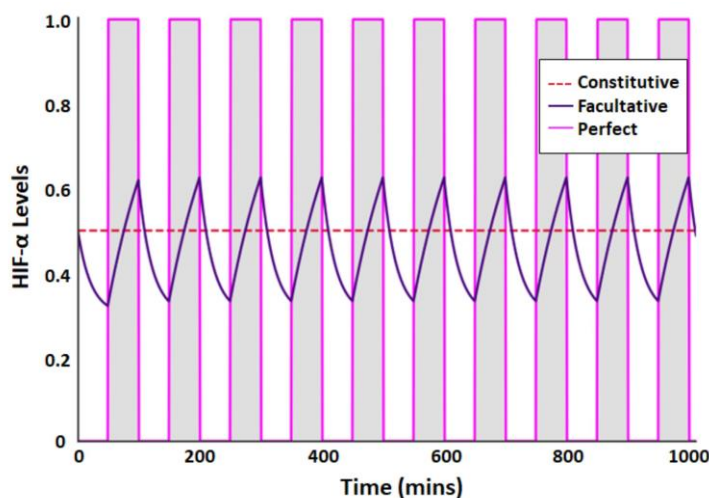451 instantaneously responding with the appropriate HIF-α expression. With constitutive regulation,

Figure 7. Comparison of 3 HIF-α response strategies to changes in oxygen supply within the tumor (cell) microenvironment. The perfect strategy is instantaneous and used as an upper bound for comparison. Constitutive is constant over time, and facultative has a rate-limited response. The unshaded areas represent periods of full oxygenation while the shaded grey areas represent periods of hypoxia.

452 HIF-α is constantly maintained at an above baseline level regardless of the O_2 levels. With
453 facultative regulation, HIF-α levels change in response to environmental fluctuations in oxygen at
454 fixed rates of accumulation (slow) and degradation (fast). It is important to note that we use "HIF-
455 α" to represent the constellation of cellular responses to hypoxia. While the transcription factor
456 HIF-1α is undoubtedly central to this, we do not wish to imply that its levels are solely responsible
457 for a cell's fitness under different conditions of oxygenation.
458
459 **Environment creation**
460 Let $Y \in [0, 1]$, describe the level of oxygenation in the cell's tumor microenvironment. In all
461 scenarios, we assume that the environmental switch between fully oxygenated ($Y=1$) or
462 deoxygenated ($Y=0$) is effectively instantaneous whereas the accumulation and degradation of
463 HIF-α is based on intrinsic rates. Let $u(t)$ be the HIF-α response of a cell at time t whether it has a
464 perfect, constitutive, or facultative response, where $u \in [0, 1]$. For the fixed interval environment,
465 normoxic ($Y=1$) and hypoxic ($Y=0$) periods switch back and forth at fixed time intervals. A
466 perfect, constitutive, and facultative response to these changing oxygen profiles will exhibit
467 different HIF-α expression levels. (Fig. 7).
468
469 **The perfect strategy**
470 With the perfect strategy, the switching response to the environment is instantaneous. Therefore,
471 $u=0$ during periods of normoxia and $u=1$ during periods of hypoxia. We can thus simply take the
472 sum of the payoffs spent in each environment using Eq. (1), and expected payoff becomes:
473

$$G_{\text{perfect}} = r_0 - (1 - q)\left(c + \frac{m}{k+b}\right) \tag{2}$$

475

14

476
477 **The constitutive strategy**
478 With the constitutive strategy, HIF-α levels remain constant and do not change in response to the
479 temporal fluctuations in oxygen. When u is fixed, the expected payoff for the constitutive HIF-α
480 strategy can be separated into the payoff during normoxia, $G_N(u) = r - cu$, and the payoff during
481 hypoxia, $G_H(u) = r - cu - m(1-q)/(k+bu)$, so that the total payoff is:
482

483
$$G = qG_N(u) + (1 - q)G_H(u) = r - cu - \frac{(1-q)^2 m}{k+bu}.$$

484
485 The optimal value for HIF-α expression depends only on the fraction of time spent in each state,
486 q. Therefore, the optimal constitutive strategy value, u^*, can be calculated analytically by
487 maximizing expected G with respect to u. We take the first order necessary condition for this
488 optimum, $\frac{dG}{du} = 0$, and solve for u*, resulting in:
489

490
$$u^* = \sqrt{\frac{m(1-q)}{bc}} - \frac{k}{b}. \tag{3}$$

491
492
493 The constitutive level of HIF-α production declines with its proliferation cost, c, the cell's intrinsic
494 tolerance to hypoxia in the absence of HIF-α stabilization, k, and the fraction of time spent
495 normoxic, q. HIF-α production increases with cell mortality when conditions are hypoxic, m. The
496 relationship between optimal HIF-α production and the benefit of HIF-α expression u in reducing
497 mortality when conditions are hypoxic, b, is hump shaped. If HIF-α expression is ineffective (small
498 b) then there is no point, and if HIF-α expression is extremely effective (large b) then little is
499 needed. The u^* can then be substituted into the payoff G to determine the maximal payoff
500 available to the constitutive strategy given the micro-environmental and fitness parameters:
501

502
$$G^* = r_0 - \sqrt{1-q}\left(c + \frac{m}{k+b}\right) - \frac{ck}{b}\left(\sqrt{1-q} - 1\right). \tag{4}$$

503
504 **The facultative strategy**
505 Under the facultative strategy, when the environment is depleted of oxygen, we assume that the
506 cell accumulates HIF-α at a finite rate α_0, and when the environment is fully oxygenated the cell
507 degrades HIF-α at a finite rate α_1 (1). We allow a baseline production of HIF-α (u_{min}) even under
508 normal oxygen conditions and assume that the cell targets a maximum accumulation of HIF-α
509 (u_{max}) in an oxygen-depleted environment (2). We assume that the changes in expression occur
510 at a rate proportional to the difference between some desired level and the current level, such
511 that:
512

513
$$\frac{du}{dt} = \begin{cases} \alpha_0(u_{max} - u) & \text{if Y=0} \\ -\alpha_1(u - u_{min}) & \text{if Y=1} \end{cases} \tag{5}$$

514
515 For the facultative strategy, the dynamic $u(t)$ requires that the expected payoff be calculated as the
516 cumulative payoff over the normoxic and hypoxic periods, T_N and T_H, respectively. Because the
517 HIF-α fluctuations become periodic, the total cumulative payoffs can be averaged over a cycle
518 separated into the time spent in normoxia and the time spent in hypoxia:

15

519

$$G = \frac{\int_0^{T_N} G_N(u) + \int_0^{T_H} G_H(u)}{T_N + T_H}.$$

520
521 The payoff can be analytically solved to:

522

$$G = r - \frac{c}{T}(u_{min}T_N + u_{max}T_H) + \frac{c\beta_N\beta_H(u_{max}-u_{min})(\alpha_1-\alpha_0)}{\alpha_0\alpha_1\beta T} +$$

523

524 $$\frac{m}{\alpha_0(k+bu_{max})T}\ln\left|\frac{k\beta + b[u_{min}\beta_N + u_{max}\beta_H e^{-\alpha_1 T_N}]}{k\beta e^{\alpha_0 T_H} + b[u_{min}\beta_N + u_{max}\beta_H e^{\alpha_0 T_H}]}\right|, \qquad (6)$$

525

526 where $T=T_N+T_H$, $\beta = 1 - e^{-\alpha_0 T_H - \alpha_1 T_N}$, $\beta_N = 1 - e^{-\alpha_1 T_N}$, and $\beta_H = 1 - e^{-\alpha_0 T_H}$. The derivation
527 is provided in the supplemental material.

528

529 The payoff for the facultative HIF-α strategy in a stochastic environment is calculated similarly.
530 But, because the HIF-α dynamics cannot settle into a dynamic equilibrium, the payoff is calculated
531 over discretized time intervals and then taken as an average over the entire simulation.

532

533 **Finding the optimal u*_{min} and u*_{max} for the facultative strategy**
534 Constrained optimization by linear approximation (COBYLA) was used to determine values of
535 u^*_{min} and u^*_{max} that maximize a cell's payoff. For stochastic environments, a search space was
536 created by linearly separating 250 values between 0 and 1. These values were used to create
537 combinations of u_{min} and u_{max} for which $0 \le u_{min} < u_{max} \le 1$. After $u(t)$ was computed for each
538 combination of u_{min} and u_{max}, the payoff, $G(u(t))$, was calculated as an average of all payoff values
539 at each time point. The combination of u_{min} and u_{max} that produced the maximum averaged payoff
540 was considered optimal. For a given $P_{N \to H} = P_{H \to N}$, we ran 10 replicate runs for 2000 time units.
541 With this number of time units, the estimated values of u^*_{min} and u^*_{max} were very similar across
542 replicate runs (standard error of the mean < 0.01).

543

544 **Selection coefficient for facultative expression**
545 We define the selection coefficient (SC) as the fitness advantage for using a facultative rather than
546 a constitutive strategy. We calculated the SC as the difference between the payoff for facultative
547 expression, G_F, and the payoff for constitutive expression, G_C, normalized by the payoff for
548 constitutive expression, $SC=(G_F-G_C)/G_C$.

549

550 **Cell lines and Culture Conditions**
551 A2780s and TOV112D ovarian cancer cells were obtained through American Type Culture
552 Collection (ATCC). Cells were grown in RPMI supplemented with 10% fetal bovine serum (FBS).
553 For both normoxic and hypoxic treatment environments, all cells were grown in 5% CO_2 and at
554 37°C in a humidified atmosphere.

555

556 **Stabilization/degradation of HIF**
557 A Biospherix X-Vivo Hypoxia Chamber was used to incubate cells under hypoxic conditions. For
558 hypoxic conditions, cells were incubated at 0.2% O_2:94.8% N_2:5% CO_2. Reoxygenation was
559 performed by transferring flasks or plates containing cells from the hypoxic chamber to an
560 incubator under atmospheric conditions at 5% CO_2. For time points shorter than 4 hours, media

561 pre-equilibrated under hypoxic conditions was used. Then, the hypoxic media was added to the
562 cells inside a hypoxic (0.2% O_2) working chamber within the Biospherix complex.
563
564 **Western blot analyses**
565 Western blots were performed on A2780 and TOV112D ovarian cancer cells to validate the
566 expression of HIF at the protein level at different time points. Cells grown in hypoxic chambers
567 were frozen at the time points mentioned in the results section and harvested all together by lysing
568 in Radioimmunoprecipitation assay buffer (RIPA buffer) containing 1× protease inhibitor cocktail
569 (Sigma-Aldrich). For each sample, a 30 µg aliquot was loaded onto pre-cast polyacrylamide-SDS
570 gels from BioRAd that were then transferred onto nitrocellulose. Membranes were incubated with
571 primary antibodies against HIF-1α (#610958, BD Biosciences), Tubulin (#2144, CST) or β-Actin
572 (A5441, Sigma, 1:4000) overnight at 4° C, followed by fluorescent-conjugated secondary
573 antibodies (IRDye® 800CW Goat anti-MouseIgG and IRDye® 8680CW Goat anti-rabbit IgG). An
574 Odyssey chemiluminescence-fluorescence system was used for protein detection. Proteins
575 detected ran at the expected molecular weights, as verified using molecular weight standard
576 markers.
577
578 **MRI tumor imaging of hypoxia**
579 *In vivo* measurements of oxygenation fluctuations were obtained by Intrinsic Susceptibility
580 Magnetic Resonance Imaging (IS-MRI)[50]. Panc02 mouse pancreatic adenocarcinoma cells were
581 implanted subcutaneously into a C57BL/6 mouse. When the tumor reached a volume of
582 ~1500mm^3, as measured by calipers, the animal underwent MR imaging with a 7T/30cm Bruker
583 Biospec® imaging spectrometer as follows. Mice were anaesthetized using 3% isoflurane and
584 subsequently maintained with 1.5-2% isoflurane mixed with 100% oxygen. Anatomical images
585 were acquired using T2-weighted coronal and axial scans to identify the middle of the tumor and
586 facilitate outlining the tumor. To capture the spatial and temporal dynamics of oxygenation,
587 quantitative T2* mapping was then performed continuously every 55s for 18 series (Multi-
588 Gradient Echo, TR=270ms, 10xTE=2.5-47.5ms, flip angle 40 degrees, 5 slices, 1mm/1mm slice
589 thickness/gap, 35mm FOV, 128x128 points). A monoexponential function was fitted for each
590 voxel at each time-point (MATLAB 2018b, Mathworks) to reconstruct the local T2* magnetic
591 resonance time, which is modulated by changes in deoxyhaemoglobin levels in the blood, hence
592 reflecting the fluctuations in blood oxygen level.
593
594 **Acknowledgements**
598
599
600 **Author contributions**
601 R.J.G., J.S.B., and C.J.W. conceived of and designed the research. M.P., J.A.G. and J.S.B.
602 performed the mathematical modeling. M.R.T., M.D. and P.B. conducted the laboratory work.
603 M.P., J.A.G, and C.J.W. wrote the manuscript, and M.P, J.A.G., J.S.B., M.R.T., M.D., R.J.G. and
604 C.J.W. revised the manuscript.
605
606 **Additional information**
607 **Competing interests:** The authors declare no conflicts of interest.

References

1. Pigliucci M. Phenotypic plasticity: beyond nature and nurture. (The John Hopkins University Press, 2001).

2. Dekel E, Alon U. Optimality and evolutionary tuning of the expression level of a protein. *Nature* **436**, 588 (2005).

3. López-Maury L, Marguerat S, Bähler J. Tuning gene expression to changing environments: from rapid responses to evolutionary adaptation. *Nat Rev Genetics* **9**, 583-93 (2008).

4. Stamp N. Out of the quagmire of plant defense hypotheses. *Quart Rev Biol* **78**, 23-55 (2003).

5. Geisel N. Constitutive versus responsive gene expression strategies for growth in changing environments. *PLoS ONE* **6**, e27033. doi:10.1371/journal.pone.0027033 (2011).

6. Adler FR, Harvell CD. Inducible defenses, phenotypic variability and biotic environments. *Trends Ecol & Evol* **5**, 407-10 (1990).

7. Harvell CD. The ecology and evolution of inducible defenses *Quart Rev Biol* **65**, 323-40 (1990).

8. Forsman, A. Rethinking phenotypic plasticity and its consequences for individuals, populations and species. *Heredity* **115**, 276 (2015).

9. McKeown SR. Defining normoxia, physoxia, and hypoxia in tumours – implications for treatment response. *Brit J Radiol* **87**, 20130676 (2014).

10. Adamovich Y, Ladeuix B, Sobel J, Manella G, Neufeld-Cohen A, Assadi MH, Golik M, Kuperman Y, Tarasiuk A, Koeners MP, Asher G. Oxygen and carbon dioxide rhythms are circadian clock controlled and differentially directed by behavioral signals. *Cell Metab* **29**, 1092-103 (2019).

11. Brown JM, Wilson RW. Exploiting tumour hypoxia in cancer treatment. *Nat Rev Cancer* **4**, 437- 47 (2004).

12. Dewhirst MW, Cao Y, Moeller B. Cycling hypoxia and free radicals regulate angiogenesis and radiotherapy response. *Nat Rev Cancer* **8**, 425-37 (2008).

13. Dewhirst MW. Relationships between cycling hypoxia, HIF-1, angiogenesis and oxidative stress. *Radiation Res* **172**, 653-65 (2009).

14. Cárdenas-Navia LI, Mace D, Richardson RA, Wilson DF, Shan S, Dewhirst MW. The pervasive presence of fluctuating oxygenation in tumors. *Cancer Res* **68**, 5812-19 (2008).

15. Gillies RJ, Brown JS, Anderson ARA, Gatenby RA. Eco-evolutionary causes and consequences of temporal changes in intratumoural blood flow. *Nat Rev Cancer* **18**, 576–85 (2018).

16. Vaupel P, Harrison L. Tumor hypoxia: causative factors, compensatory mechanisms, and cellular response. *Oncologist* **9**, 4-9 (2004).

17. Kaelin Jr. WG, Ratcliffe, PJ. Oxygen sensing by metazoans: the central role of the HIF hydroxylase pathway. *Mol Cell* **30**, 393-402 (2008).

18. Majmundar AJ, Wong WJ, Simon MC. Hypoxia-inducible factors and the response to hypoxic stress. *Mol Cell* **40**, 294-309 (2010).

19. Samanta D, Semenza GL. Metabolic adaptation of cancer and immune cells mediated by hypoxia-inducible factors. *BBA-Reviews on Cancer* **1870**, 15-22 (2018).

20. Saxena K, Jolly MK. Acute vs. Chronic vs. Cyclic Hypoxia: Their differential dynamics, molecular mechanisms, and effects on tumor progression. *Biomolecules* **9**, 339 (2019).

18

21. Goda N, Ryan HE, Khadivi B, McNulty W, Rickert RC, Johnson RS. Hypoxia-inducible factor 1α is essential for cell cycle arrest during hypoxia. *Mol Cell Biol* **23**, 359-69 (2003).

22. Liu L, Cash TP, Jones RG, Keith B, Thompson CB, Simon MC. Hypoxia-induced energy stress regulates mRNA translation and cell growth. *Mol Cell* **21**;521-31 (2006).

23. Hickey MM, Simon MC. Regulation of angiogenesis by hypoxia and hypoxia inducible factors. *Curr Topics Devel Biol* **76**, 217-57 (2006).

24. Tan CC, Ratcliffe PJ. Effect of inhibitors of oxidative phosphorylation on erythropoietin mRNA in isolated perfused rat kidneys. *Amer J Phys-Renal Phys* **261**, F982-F987 (1991).

25. Gleadle JM, Ratcliffe PJ. Induction of Hypoxia-Inducible Factor-1, Erythropoietin, Vascular Endothelial Growth Factor, and Glucose Transporter-1 by Hypoxia: Evidence Against a Regulatory Role for Src Kinase. *Blood* **89**, 503-09 (1997).

26. Semenza GL. Involvement of oxygen-sensing pathways in physiologic and pathologic erythropoiesis. *Blood* **114**, 2015-19 (2009).

27. Russell S, Gatenby RA, Gillies RJ, Ibrahim-Hashim A. Pseudohypoxia: Life at the Edge. in Ecology and Evolution of Cancer, (eds. Ujvari, B, Roche, B., Thomas, F.) 57-68 (Academic Press, 2017).

28. Kim JW, Dang CV. Cancer's molecular sweet tooth and the Warburg effect. *Cancer Res* **66**, 8927-30 (2006).

29. Liberti MV, Locasale JW. The Warburg effect: how does it benefit cancer cells? *Trends Biochem Sci* **41**;211-18 (2016).

30. Pastorekova S, Gillies RJ. The role of carbonic anhydrase IX in cancer development: links to hypoxia, acidosis, and beyond. *Cancer Metas Rev* **38,** 65-77 (2019).

31. Lee S.H, McIntyre D, Honess D, Hulikova A, Pacheco-Torres J, Cerdán S, Swietach P, Harris AL, Griffiths JR. Carbonic anhydrase IX is a pH-stat that sets an acidic tumour extracellular pH in vivo. *British J Cancer* **119**, 622-30 (2018).

32. Rhoades DF. Evolution of plant chemical defense against herbivores, in Herbivores: Their interaction with secondary plant metabolites, (eds. Rosenthal, GA, Janzen, DH) 3-54 (Academic Press, 1979).

33. Pagé EL, Robitaille GA, Pouysségur J, Richard DE. Induction of hypoxia-inducible factor-1α by transcriptional and translational mechanisms. *J Biol Chem* **277**, 48403-09 (2002).

34. Marxsen JH, Stengel P, Doege K, Heikkinen P, Jokilehto T, Wagner T, Jelkmann W, Jaakkola P, Metzen E. Hypoxia-inducible factor-1 (HIF-1) promotes its degradation by induction of HIF-α-prolyl-4-hydroxylases. *Biochem Journal* **381**, 761-67 (2004).

35. Foley R, Marignol L, Thomas AZ, Cullen IM, Perry AS, Tewari P, O'Grady A, Kay E, Dunne B, Loftus B, Watson RW. The HIF-1α C1772T polymorphism may be associated with susceptibility to clinically localized prostate cancer but not with elevated expression of hypoxic biomarkers. *Cancer Biol & Therapy* **8**, 118-24 (2009).

36. Graham AM, Barreto FS. Loss of the HIF pathway in a widely distributed intertidal crustacean, the copepod *Tigriopus californicus*. *Proc. Natl Acad. Sci. USA* **116**, 12913-18 (2019).

37. Mills DB, Francis WR, Vargas S, Larsen M, Elemans CP, Canfield DE, Wörheide G. The last common ancestor of animals lacked the HIF pathway and respired in low-oxygen environments. *Elife* **7**, e31176 (2018).

38. Graham AM, Presnell JS. Hypoxia Inducible Factor (HIF) transcription factor family expansion, diversification, divergence and selection in eukaryotes. *PLoS ONE* **12**, e0179545. https://doi.org/10.1371/journal.pone.0179545 (2017).

39. Bell, A. Early work on periodic motion. *Nature* **147** (3716), 78–80 (1941).

40. Hardy KM, Follett CR, Burnett LE, Lema SC. Gene transcripts encoding hypoxia-inducible factor (HIF) exhibit tissue-and muscle fiber type-dependent responses to hypoxia and hypercapnic hypoxia in the Atlantic blue crab, Callinectes sapidus. *Comp Biochem Physiol Part A: Mol Integrative Phys* **163**, 137-46 (2012).

41. Ratcliffe PJ. Oxygen sensing and hypoxia signalling pathways in animals: the implications of physiology for cancer. *J Phys* **591**, 2027-42 (2013).

42. Ramirez JM, Folkow LP, Blix AS. Hypoxia tolerance in mammals and birds: from the wilderness to the clinic. *Ann RevPhys* **69**, 113-43 (2007).

43. Cavadas MA, Nguyen LK, Cheong A. Hypoxia-inducible factor (HIF) network: insights from mathematical models. *Cell Comm Signaling* **11**, 42 (2013).

44. Kohn KW, Riss J, Aprelikova O, Weinstein JN, Pommier Y, Barrett JC. Properties of switch-like bioregulatory networks studied by simulation of the hypoxia response control system. *Mol Biol Cell* **15**, 3042-52 (2004).

45. Qutub AA, Popel AS. A computational model of intracellular oxygen sensing by hypoxia-inducible factor HIF1 alpha. *J Cell Sci* **119**, 3467–80 (2006).

46. Yucel MA, Kurnaz IA. An in silico model for HIF-α regulation and hypoxia response in tumor cells. *Biotech Bioeng* **97**, 588-600 (2007).

47. Schmierer B, Novak B, Schofield CJ. Hypoxia-dependent sequestration of an oxygen sensor by a widespread structural motif can shape the hypoxic response–a predictive kinetic model. *BMC Systems Biol* **4**, 139 (2010).

48. Nguyen LK, Cavadas MA, Scholz CC, Fitzpatrick SF, Bruning U, Cummins EP, Tambuwala MM, Manresa MC, Kholodenko BN, Taylor CT, Cheong, A. A dynamic model of the hypoxia-inducible factor 1-alpha (HIF-1alpha) network. *J Cell Sci* **126**, 1454–63 (2013).

49. Gatenby RA, Gawlinski ET, Gmitro AF, Kaylor B, Gillies RJ. 2006. Acid-mediated tumor invasion: a multidisciplinary study. *Cancer Res* **66**, 5216-23 (2006).

50. Robinson SP, Rijken PF, Howe FA, McSheehy PM, van der Sanden BP, Heerschap A, Stubbs M, van der Kogel AJ, Griffiths JR. Tumor vascular architecture and function evaluated by non-invasive susceptibility MRI methods and immunohistochemistry. *J. Magn. Reson. Imaging* **17**, 445-54 (2003).